Available online at www.sciencedirect.com
SCIENCE DIRECT
Physica E 32 (2006) 167–170
PHYSICA E
www.elsevier.com/locate/physe

Scanning a metallic tip close to a quantum point contact

A. Pioda[a], D. Brunner[a], S. Kicin[a], T. Ihn[a], M. Sigrist[a,*], A. Fuhrer[a], K. Ensslin[a], M. Reinwald[b], W. Wegscheider[b]

[a]*Solid State Physics, ETH Zürich, 8093 Zürich, Switzerland*
[b]*Institut für experimentelle und angewandte Physik, Universität Regensburg, Germany*

Available online 15 February 2006

Abstract

Low-temperature transport experiments on a quantum point contact under the influence of a scanning gate are reported. The scanning gate is the metallic tip of a scanning force microscope operating at a temperature of 300 mK. In particular, the influence of the scanning tip on conductance resonances observed in the gate-characteristics of the point contact is studied. The strongest conductance resonances appear to be related to the local potential within the channel of the point contact. As a consequence, the point contact with its conductance resonances can be used as a sensor for the local tip-induced potential.

PACS: 07.20.Mc; 73.63.−b

Keywords: Scanning probe microscopy; Scanning-gate microscopy; Quantum point contact

Quantum point contacts (QPCs) are fundamental building blocks of quantum devices. Their quantized low-temperature conductance observed in very clean samples is a paradigm of the quantum transport of non-interacting electrons [1,2]. Recently, a number of low-temperature scanning gate experiments have been reported investigating the conductance of such quantum point contacts on a local scale [3,4]. A glimpse of the probability density of quantized modes was obtained [4] and the branched coherent flow of electrons injected from a QPC into a two-dimensional electron gas (2DEG) came as a complete surprise [5].

In this paper, we focus on a QPC fabricated on a slightly lower mobility 2DEG. In such systems, coherent quantum scattering in and around the QPC channel leads to resonant features in the conductance as a function of the QPC width [6]. We have investigated such resonances locally with a scanning probe technique. Scanning gate measurements were performed in the vicinity of a QPC. The observed resonances in the transmission through the QPC can be influenced with the scanning gate. The development of resonances at different tip voltages was studied. It was possible to reconstruct the tip-induced potential using the QPC conductance with its resonances as a local detector.

The QPC studied in the experiment was prepared on a GaAs/AlGaAs heterostructure. A 2DEG was buried 34 nm below the surface. Mobility 450,000 $\mathrm{cm^2/V\,s}$ and electron density $5\times10^{11}\,\mathrm{cm^{-2}}$ of the 2DEG were determined at a temperature of 4.2 K. A mesa was fabricated by wet chemical etching in the first processing step. Subsequently, the QPC and other quantum structures were defined using local anodic oxidation of the GaAs surface with a room temperature scanning force microscope (SFM) [7]. Fig. 1a shows the resulting topography of the surface. The 2DEG is depleted below the bright oxide lines. The QPC is formed below a 180 nm gap between two orthogonal oxide lines. The transmission of the QPC can be tuned by the in-plane gate. The other structures defined in the vicinity of the QPC will not be discussed in this paper.

The experiments were performed with a low-temperature SFM in an ^{3}He cryostat with a base temperature of 300 mK. The electron temperature was estimated from transport measurements on the neighboring quantum dot structure to be about 550 mK. A tuning fork sensor with an

*Corresponding author.
E-mail address: msigrist@phys.ethz.ch (M. Sigrist).

1386-9477/$ - see front matter © 2006 Elsevier B.V. All rights reserved.
doi:10.1016/j.physe.2005.12.124

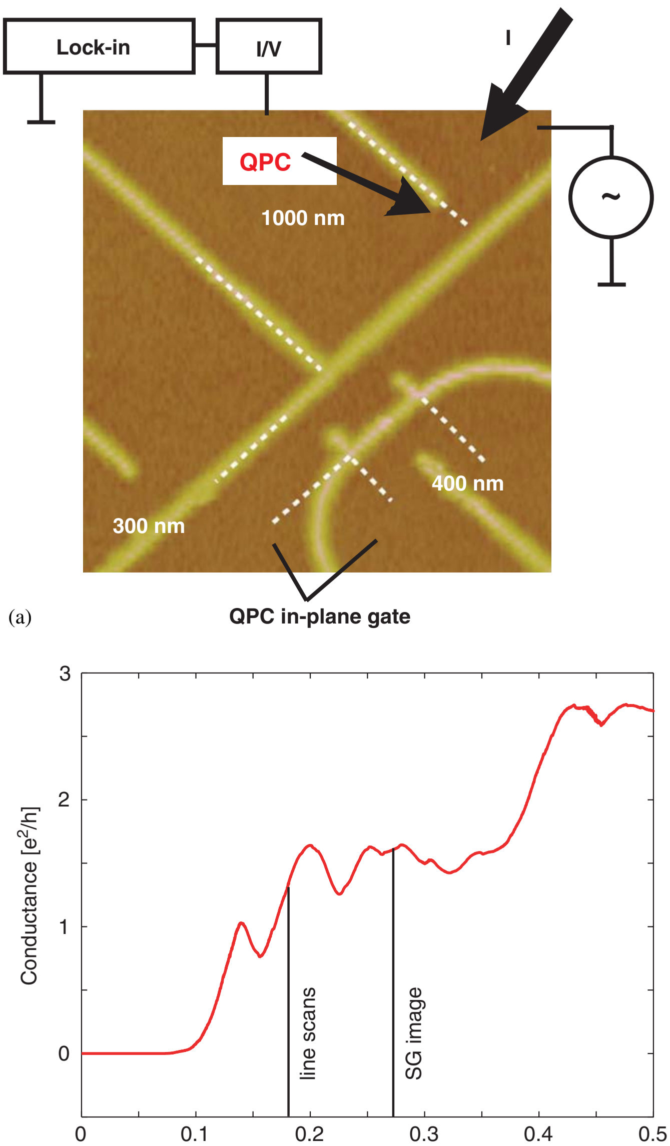

Fig. 1. (a) Topography of the structure with the QPC measured with an AFM at room temperature. In addition to the QPC under investigation, a quantum dot can be seen. The two-terminal measurement set-up is schematically indicated. (b) Conductance of the QPC as a function of the voltage V_{IG} on the in-plane gate with the scanning tip fully withdrawn.

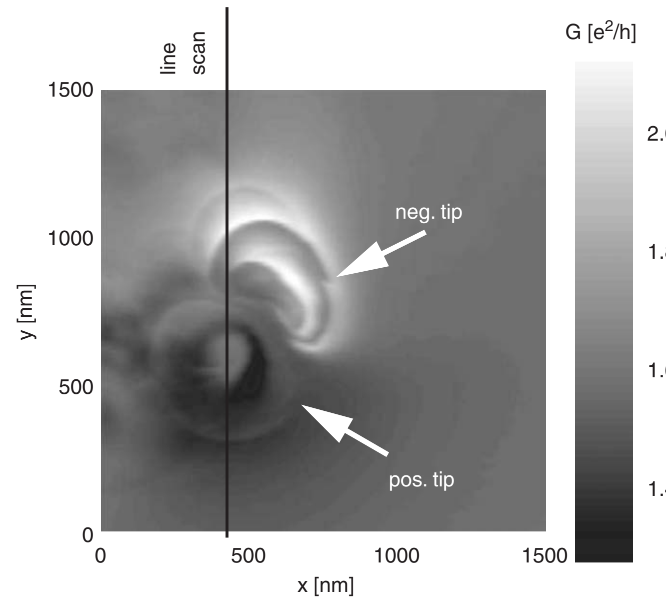

Fig. 2. Scanning gate image obtained at the gate voltage indicated in Fig. 1b. Two sets of fringes are indicated by arrows. The line marked "line scan" indicates where the line scans shown in Fig. 3 were performed.

electrochemically sharpened metallic PtIr tip was scanned at constant height above the surface during the experiment. Because it is capacitively coupled to the 2DEG, it can be considered as a scanning gate. An AC bias of 100 μV was applied across the QPC at a frequency of 81.3 Hz. A two-terminal set-up (contact resistance about 3.6 kΩ) and a lock-in technique were used to measure the current through the QPC. The current was recorded on a grid of tip positions. The resulting scanning gate images are maps of the tip-position dependent QPC conductance.

Fig. 1b shows the conductance of the QPC with the tip fully withdrawn as a function of the voltage V_{IG} on the in-plane gate. At voltages below 0.1 V the conductance is completely suppressed. The rise to the first conductance plateau observed for increasing V_{IG} is decorated with reproducible transmission resonances typical for the conductance of QPCs fabricated on 2DEGs with moderate mobility. They are commonly believed to arise from coherent scattering in the 1D channel and in its vicinity.

In our first scanning experiment the in-plane gate was used to tune the conductance of the QPC to the center of the first conductance plateau, with the tip far away from the QPC. Fig. 2 shows a scanning gate image obtained by keeping the tip on a plane 100 nm above the sample surface. A voltage of 600 mV was applied on the tip. Two sets of fringes can be observed in Fig. 2. They can be attributed to transmission resonances in the QPC as observed in the plunger-gate dependence of the QPC conductance. While one set of fringes comes along with a general increase of the QPC conductance, the other set goes with strongly reduced conductance. The appearance of two sets of fringes is, however, beyond naive expectations and requires further measurements.

In order to follow the evolution of the fringes with varying tip voltages we therefore performed series of line scans of 1.7 μm length, as indicated by the black line in Fig. 2. The tip-sample separation was reduced to 60 nm. The QPC conductance was tuned (with the tip far remote) to the onset of the first conductance plateau using the in-plane gate. The tip voltage was varied between −0.1 and 1 V. The results are presented in Fig. 3a.

The figure shows a grayscale image of the QPC conductance measured as a function of tip position along the line and tip voltage. For all tip voltages, a region of reduced conductance around −1400 nm and a region of enhanced conductance around −600 nm can be identified.

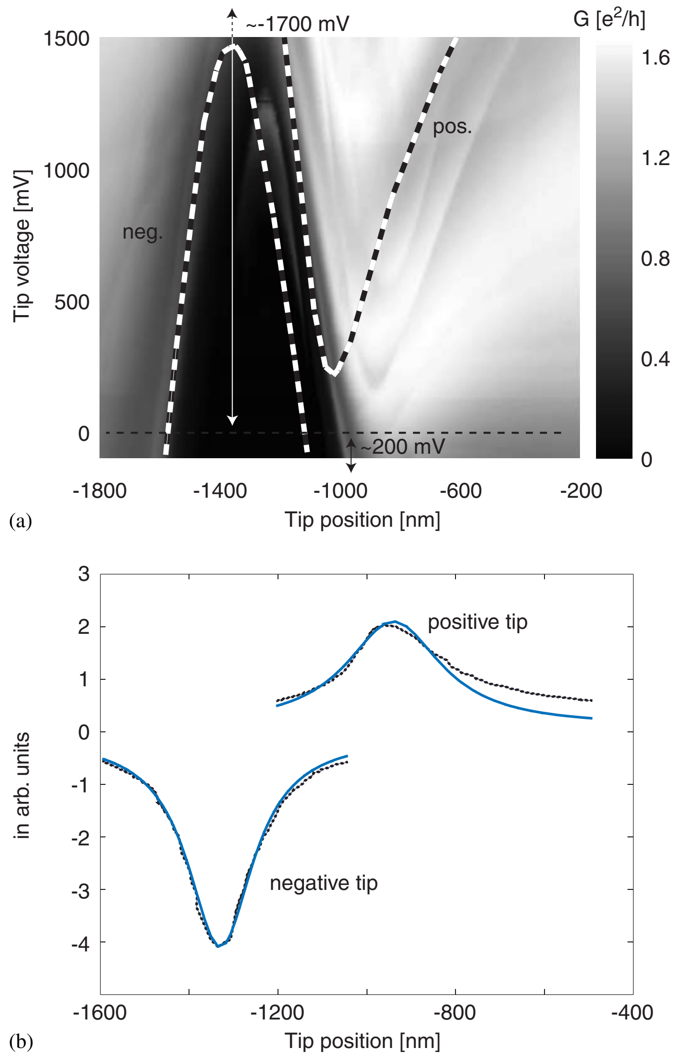

Fig. 3. (a) Gray scale image of the QPC conductance as a function of tip position along the line indicated in Fig. 2 and tip voltage. (b) The two contributions to the tip-induced potential discussed in the text (dashed). The data has been fitted with Lorentzians (solid curves).

These two regions correspond to the reduced and enhanced conductance regions associated with the two sets of resonance fringes in Fig. 2.

Fine filamentary lines of parabolic shape accompany the enhanced and reduced conductance regions. They correspond to the fringes in Fig. 2 associated with resonances of the QPC conductance. The behavior of the two sets of filaments is directly opposed—while that coming with the region of reduced conductance shows a parabolic shape with opening to low tip voltages, the other one shows a similar shape with opening to high tip voltages.

The effect of the tip on the transmission of the QPC is manifold. In the simplest empirical picture, the tip-induced potential will shift the energies of quantized modes, i.e., the tip acts like an additional gate electrode. We call this effect *gating effect* of the tip. The resulting QPC conductance can be expressed as the gate voltage characteristic $G(V_{\mathrm{IG}})$ shifted by the effective tip-induced potential in the QPC constriction, i.e.,

$$G(\vec{r}) = G[V_{\mathrm{IG}} + \alpha(\vec{r})(V_{\mathrm{tip}} - V_{\mathrm{CPD}})]. \tag{1}$$

Here, the characteristic function $\alpha(r)$ is proportional to the tip-induced potential in the 2DEG, and V_{CPD} is an offset voltage arising due to the contact potential difference between the tip material and the heterostructure. This effect is the QPC-analogue to scanning gate experiments on quantum dots in the Coulomb blockade regime, where a shift in quantum dot energy levels can be directly detected as conductance resonance fringes in scanning gate images [8].

The tip-induced potential $\alpha(r)$ can be obtained from the measurement shown in Fig. 3a by tracking lines of constant QPC conductance or, alternatively, by tracking some of the filamentary resonances. From Eq. (1) we obtain

$$\alpha(\vec{r}) \propto 1/(V_{\mathrm{tip}} - V_{\mathrm{CPD}}).$$

The two black curves in Fig. 3a suggest that the spatial dependence of $\alpha(r)$ does not only exhibit a single maximum, but rather the combination of a maximum and a minimum. In addition, the contact potential difference involved for the two extremes are apparently different. We estimate from our data the two values $V_{\mathrm{CPD1}} = -1.7\,\mathrm{V}$ and $V_{\mathrm{CPD2}} = +0.2\,\mathrm{V}$. In Fig. 3b we plot the two parts $\alpha_i(r)$ of the total $\alpha(r) = \alpha_1(r) + \alpha_2(r)$. Both experimental curves can be fitted reasonably well with Lorentzians.

The total tip-induced potential in our experiment is, therefore, the superposition of two approximately Lorentzian-shaped contributions which are spatially separated. One part

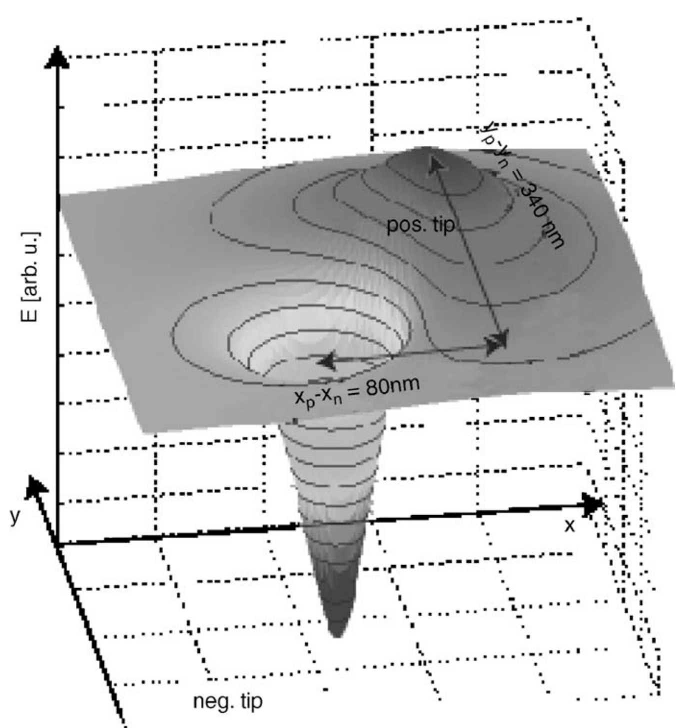

Fig. 4. Tip-induced energy shift at zero tip bias as reconstructed from two orthogonal line scans like the one shown in Fig. 3a. The double-tip discussed in the text manifests itself in the attractive and repulsive contributions to the energy shift.

of the potential is repulsive while the other is attractive. This behavior is also found in the scanning gate image presented in Fig. 2, where one set of fringes is seen around a region of suppressed conductance, while the other set is found in a region of enhanced conductance. The most reasonable explanation for the observed tip-induced potential is a double-tip, one part of which consists of a different material than the other, as suggested by the two different values of the contact potential difference.

Performing the analysis sketched above for tip-voltage dependent line scans in two orthogonal spatial directions leads to an approximate 2D map of the tip-induced potential. The associated shift of quantized mode energies ΔE in the QPC can then be reconstructed from

$$\Delta E \propto \alpha_1(\vec{r})(V_{\mathrm{tip}} - V_{\mathrm{CPD1}}) + \alpha_2(\vec{r})(V_{\mathrm{tip}} - V_{\mathrm{CPD2}}).$$

The result of this analysis is shown in Fig. 4 for $V_{\mathrm{tip}} = 0\,\mathrm{V}$.

In addition to the gating effect discussed above, the tip-induced potential can influence the 2DEG via phase-coherent interference effects. The measured conductance is altered by additional backscattering induced by the tip, a mechanism which is inherently non-local. Furthermore, the tip-induced potential can cause discrete charge rearrangements in the vicinity of the QPC which are detected as changes in the QPC conductance. These effects existing in addition to the gating effect go beyond the scope of this paper and will be discussed elsewhere [9].

In conclusion, we have shown a scanning gate experiment on a quantum point contact defined by local anodic oxidation on a Ga[Al]As heterostructure. From the data we were able to isolate a direct gating effect of the tip measured via the conductance of the point contact. A double tip consisting of two different materials was identified, and its induced potential was qualitatively mapped in 2D.

References

[1] B.J. van Wees, H. van Houten, C.W.J. Beenakker, J.G. Williamson, L.P. Kouwenhoven, D. van der Marel, C.T. Foxon, Phys. Rev. Lett. 60 (1988) 848.

[2] D.A. Wharam, T.J. Thornton, R. Newbury, M. Pepper, H. Ahmed, J.E.F. Frost, D.G. Hasko, D.C. Peacock, D.A. Ritchie, G.A.C. Jones, J. Phys. C 21 (1988) 209.

[3] M.A. Topinka, B.J. LeRoy, S.E.J. Shaw, E.J. Heller, R.M. Westervelt, K.D. Maranowski, A.C. Gossard, Science 289 (2000) 2323.

[4] R. Crook, C.G. Smith, M.Y. Simmons, D.A. Ritchie, J. Phys.: Condens. Matter 12 (2000) L735.

[5] M.A. Topinka, B.J. LeRoy, R.M. Westervelt, S.E.J. Shaw, R. Fleischmann, E.J. Heller, K.D. Maranowski, A.C. Gossard, Nature (London) 410 (2001) 183.

[6] B.J. van Wees, L.P. Kouwenhoven, E.M.M. Willems, C.J.P.M. Harmans, J.E. Moolij, H. van Houten, C.W.J. Beenakker, J.G. Williamson, C.T. Foxon, Phys. Rev. B 43 (1991) 012431.

[7] A. Fuhrer, A. Dorn, S. Lüscher, T. Heinzel, K. Ensslin, W. Wegscheider, M. Bichler, Superlattices Microstruct. 31 (2002) 19.

[8] A. Pioda, S. Kicin, T. Ihn, M. Sigrist, A. Fuhrer, K. Ensslin, A. Weichselbaum, S.E. Ulloa, M. Reinwald, W. Wegscheider, Phys. Rev. Lett. 93 (2004) 216801.

[9] A.Pioda, D. Brunner, S. Kicin, T. Ihn, K. Ensslin, to be published.